

# New Gamma-Ray Bursts Found in the Archival Data from the IBIS/ISGRI Telescope of the INTEGRAL Observatory

I. V. Chelovekov\*, S. A. Grebenev, A. S. Pozanenko, and P. Yu. Minaev

*Space Research Institute, Russian Academy of Sciences, Profsoyuznaya ul. 84/32, Moscow, 117997 Russia*

Received November 16, 2018; revised November 24, 2018; accepted November 28, 2018

**Abstract** — A systematic search for cosmic gamma-ray bursts (GRBs) and other short hard X-ray events in the archival data from the IBIS/ISGRI telescope of the INTEGRAL observatory over 2003–2018 has been carried out. Seven previously unknown GRBs have been recorded in the telescope field of view; all of them have been localized with an accuracy  $\leq 2$  arcmin. These events were not revealed by the INTEGRAL burst alert system (IBAS) designed for an automatic GRB search and alert. Four more such localized events missed by IBAS, but known previously, i.e., observed in other experiments, have been found. Eight hundred and eighty six GRBs outside the field of view that arrived at large angles to the IBIS/ISGRI axis have also been recorded. All of them were previously recorded in other experiments, primarily by the anticoincidence shield (ACS) of the SPI gamma-ray spectrometer onboard the INTEGRAL observatory, the PICsIT detector of the IBIS gamma-ray telescope, and the KONUS/WIND monitor. An order of magnitude more events without any confirmations in other experiments have been recorded. Both GRBs and solar flares or magnetospheric transient events can be among them. Catalogs with the basic parameters of confirmed and previously unknown cosmic GRBs recorded by the IBIS/ISGRI telescope have been compiled. The statistical distributions of bursts in various parameters have been constructed and investigated.

**DOI:** 10.1134/S1063773719100025

**Keywords:** gamma-ray bursts, transient events.

## INTRODUCTION

Cosmic gamma-ray bursts (GRBs) have topped the list of the most puzzling, unusual astronomical phenomena for decades. Although the fact that such bursts are among the manifestations of supernova explosions may now be deemed proven, many of their properties still have no satisfactory explanation. It has become obvious that GRBs cannot be deemed events of a homogeneous sample: short (with a duration  $T_{90} \lesssim 2$  s; see Koshut et al. 1996) bursts are associated with kilonovae that erupt due to the merger of two neutron stars (or a neutron star and a black hole); long (with  $T_{90} \gtrsim 2$  s) bursts are associated with hypernovae that erupt due to the collapse of the almost bare core of a massive star (for example, a Wolf-Rayet star) at a late stage of its evolution.

To get the correct, objective idea of the origin of bursts and the composition of their population, it is necessary to have a maximally complete sample of events for a statistical analysis that includes weak and strong bursts, hard and soft bursts, but, most importantly, all of the bursts that are admitted by the sensitivity of the instrument used for their observations. Of great interest is the sample of bursts recorded by the IBIS/ISGRI gamma-ray telescope onboard the INTEGRAL observatory with

a low flux detection threshold, a wide, but sufficiently soft (for the GRB instruments) energy range (the sensitivity is at a maximum in the 20–200 keV band), the ability to locate the bursts detected in the field of view with an accuracy of 1–2 arcmin, and a huge exposure time (almost continuous observations have lasted already for more than 16 years).

A good localization of events allows one to organize a prompt search for the optical counterparts of GRBs to study the optical and X-ray afterglows of bursts and to investigate the supernova explosions associated with them. Understanding the importance of a quick identification of bursts, even before the launch of the INTEGRAL satellite into orbit, its creators developed the INTEGRAL burst alert system (IBAS, Mereghetti et al. 2003) designed for an automatic burst search and detection in the IBIS/ISGRI data and burst alert via the Gamma-ray Coordinates Network (GCN). More than 130 GRBs have already been recorded to date (Götz et al. 2006; Vianello et al. 2009; Foley et al. 2008, 2009).

Two GRBs, GRB 060428C (Grebenev and Chelovekov 2007) and GRB 070912 (Minaev et al. 2012), that fell within the IBIS field of view, but were missed by IBAS for various reasons, were previously detected in the archival data from the IBIS/ISGRI telescope of the INTEGRAL observatory. The bursts were detected

\*e-mail: chelovekov@iki.rssi.ru

serendipitously: the first during the search for thermonuclear X-ray bursts and the second initially in the data from the SPI gamma-ray spectrometer of the same observatory and only then in the IBIS/ISGRI data. It was also recorded in the KONUS/WIND experiment (Minaev et al. 2012). In the SPI data we detected one more, previously unobserved burst, GRB 060221C (Minaev et al. 2014), but this burst was short ( $T_{90} \lesssim 2$  s) and hard, the IBIS/ISGRI telescope recorded it with a low significance, therefore, the absence of detection by IBAS was not surprising.

The idea to carry out a systematic search for missed GRBs in the long-term sky observations with the IBIS/ISGRI telescope of the INTEGRAL observatory emerged after these discoveries. The results of such an analysis (the search for bursts and their investigation) are presented in this paper.

## INSTRUMENTS AND OBSERVATIONS

The IBIS gamma-ray telescope (Ubertini et al. 2003) is one of the two main instruments onboard the INTEGRAL international astrophysical gamma-ray observatory (Winkler et al. 2003). It is designed to map the sky and to investigate the detected sources in hard X-rays and soft gamma-rays. In this paper we used data from the ISGRI detector (Lebrun et al. 2003) of the telescope sensitive at  $h\nu \lesssim 400$  keV.

Unfortunately, the other detector of the telescope, PICsIT (Labanti et al. 2003), sensitive in the energy range 0.2–10 MeV could be used to record GRBs very rarely, only when it operated in the spectral-timing (ST) mode. The localization of events was not possible in this case. Bianchin et al. (2011) analyzed the accessible data from this detector obtained from May 2006 to August 2009 and revealed 39 events, 23 of which were previously observed in other experiments.

Above we have mentioned that some GRBs were recorded onboard the INTEGRAL observatory by the SPI gamma-ray spectrometer within its field of view (see, e.g., Minaev et al. 2012, 2014). A considerably larger number of them were recorded outside the field of view of the instrument — by its anticoincidence shield (ACS) having a large effective area (the mean detection rate reached  $\sim 15$  bursts per month, Rau et al. 2005; Minaev et al. 2010; Minaev and Pozanenko 2017). In this case, in view of the peculiarities of the SPI geometry, its shield recorded virtually no bursts arriving at small angles to the telescope axis. In contrast, the PICsIT detector had the greatest sensitivity when recording bursts arriving at small angles to the axis, within the IBIS field of view. This assertion is also completely true for the ISGRI detector of this telescope. However, as we will see below, the telescope also records a large number of GRBs outside the field of view.

The principle of a coded aperture is used in the IBIS telescope to image the sky and to investigate the prop-

erties of various cosmic sources. The telescope has a  $30^\circ \times 30^\circ$  field of view (the fully coded area is  $9^\circ \times 9^\circ$ ) with an angular resolution of  $12'$  (FWHM). Such a resolution allows the positions of bright bursts to be determined with an accuracy  $\lesssim 2'$ . The sensitivity of the ISGRI detector is at a maximum in the energy range 18–200 keV. Its total area is  $2620$  cm<sup>2</sup>, the effective area for events at the center of the field of view is  $\sim 1100$  cm<sup>2</sup> (half of the detector is shielded by the opaque mask elements).

We analyzed the observational data using the standard INTEGRAL data processing software package, OSA. In searching for bursts we studied the time histories of the ISGRI detector count rates above 30 keV from February 2003 to January 2018. We analyzed a total of more than 143 000 IBIS pointings (individual sessions of its operation with a duration from half an hour to an hour), corresponding to more than 405 Ms of observations. For the burst candidates found we made an attempt to localize and identify them and then carried out their comprehensive study.

Note that by its approach and methods this study continues to some extent the series of our works (Chelovekov et al. 2006; Chelovekov and Grebenev 2011; Chelovekov et al. 2017), which is devoted to searching for thermonuclear X-ray bursts from Galactic bursters based on data of long-term observations with the JEM-X and IBIS/ISGRI telescopes of the INTEGRAL observatory. In the works of this series we analyzed the detector light curves at  $\lesssim 30$  keV. We revealed a total of 2201 bursts from known and newly detected (Chelovekov et al. 2007; Chelovekov and Grebenev 2007, 2010; Mereminskiy et al. 2017) bursters and investigated and explained some of their unusual properties (see, e.g., Grebenev and Chelovekov 2017, 2018). A complete catalog of recorded X-ray bursts and their parameters can be found at the site [dlc.rsdcrssi.ru](http://dlc.rsdcrssi.ru). Concurrently, during these works we recorded hundreds of bursts from soft gamma repeaters and erupting X-ray binary sources with highly irregular accretion.

## METHODS AND RESULTS

At the first stage of our work we investigated the time histories of the count rate for the entire IBIS/ISGRI detector (detector light curve) with a time step of 5 s in two energy ranges: 30–100 and 100–500 keV. To reveal GRB candidates, we initially found the mean count rate for a given observation (corresponding to an individual INTEGRAL pointing toward a specific sky region) and empirically determined the standard deviation of the count rate from its mean. We selected the events for which the signal-to-noise ( $S/N$ ) ratio in a time bin exceeded 3, i.e., potential GRB candidates.

For each such event we accumulated (in a time interval corresponding to its duration) and reconstructed the sky image in the IBIS field of view. If a source whose de-

**Table 1.** New GRB candidates recorded in the IBIS/ISGRI field of view, but missed by IBAS

Burst (date)	$\Delta E^a$	$T_0^b$ (UTC)	$\delta T^c$	$T_c^d$	$T_{90}^e$	$C_p^f$	$S/N^g$		$F^h$	Coordinates <sup>i</sup>	
							LC	IM		R.A.	Decl.
							hh:mm:ss	s	s	s	counts/s
GRB 041106	X	01:06:08	1	23	39	212	5.3	8.7	2496	304.749	37.295
GRB 080408C	X	18:33:54	1	21	19	669	10.4	11.5	5331	253.382	-6.694
GRB 111130	X	18:42:15	1	21	44	465	9.9	11.5	3721	345.757	48.929
	G	18:42:20	1	19	40	259	6.3	—	1604		
GRB 131107B	X	07:53:57	1	14	42	248	7.2	11.3	1794	123.378	-16.632
GRB 150803B	X	08:32:28	1	12	19	344	9.3	7.6	1776	254.055	27.121
	G	08:32:28	1	6	9	158	4.5	—	502		
GRB 160418B	X	04:20:43	5	214	179	75	3.8	7.8	1204	291.830	-44.660
GRB 161209	X	02:07:42	1	17	15	1193	17.3	26.6	9474	193.437	3.072
	G	02:07:48	1	15	25	289	4.1	—	1878		

<sup>a</sup> The energy range: X-ray  $X = 30\text{--}100$  keV and gamma-ray  $G = 100\text{--}500$  keV.

<sup>b</sup> The middle of the first bin with  $S/N > 3$  in the event profile on the detector light curve with a 5-s step.

<sup>c</sup> The time bin length in the burst light curve used to determine the burst parameters.

<sup>d</sup> The event duration on the burst light curve at 10% of the peak count rate.

<sup>e</sup> The event duration on the burst light curve estimated by the method of Koshut et al. (1996).

<sup>f</sup> The peak count rate on the unmasked burst light curve after background removal.

<sup>g</sup> The burst detection significance from the peak count rate (LC) and in the image (IM).

<sup>h</sup> The count rate integrated over the burst profile (in the time interval  $T_{90}$ ) after background removal.

<sup>i</sup> The burst coordinates from the IBIS/ISGRI data (epoch 2000.0, a radius of the  $1\sigma$ -error circle  $\sim 1'5$ ).

tection significance was no less than the event detection significance on the detector light curve ( $\gtrsim 3$  standard deviations) was revealed in the image, then the light curve was again constructed for it, this time using the tool taking into account the IBIS shadow mask (aperture) transmission for this source. If there was a significant deviation of the photon count rate recorded by the telescope from a source on the light curve coincident in time with the deviation on the detector light curve, then the event being investigated was entered into the catalog of localized GRB candidates (hereafter catalog 1). The events that were recorded on the detector light curve with a large (significant)  $S/N$  ratio, but were not detected in the corresponding image of the sky region in the IBIS field of view were not rejected, but were entered into a separate catalog (catalog 2) of GRB candidates. Both real GRBs arrived laterally, from a direction outside the IBIS field of view, and events related to solar flares, charged particles, heavy ions of cosmic origin, etc. could be among them.

The GRB candidates from catalog 1 revealed in this way were checked for a coincidence in arrival time and position in the sky with IBAS bursts. The coincident GRBs (113) were excluded from this catalog. Note that the current IBAS burst catalog<sup>1</sup> contains 131 bursts, but 13 of them were recorded outside the time interval used in this paper in searching for bursts (February 2003 – January 2018, corresponding to 40–1910 revolutions of

the INTEGRAL satellite), three bursts (GRB 050922A, GRB 091015, and GRB 091111) were too faint to be automatically detected by our method, and two more bursts (GRB 050522 and GRB 120118A) were excluded as being not GRBs. Note also that GRB 070912 (Minaev et al. 2012), which fell within the IBIS field of view, but was missed by IBAS for an unclear reason, was never included in the IBAS catalog.

The selected events from catalog 1 non-coincident with IBAS bursts were then checked (within  $\pm 50$  s) against the catalogs of bursts recorded by the SPI gamma-ray spectrometer (Minaev et al. 2012, 2014), its shield SPI/ACS<sup>2</sup>, the IBIS/PICsIT gamma-ray detector (Bianchin et al. 2011) of the INTEGRAL observatory as well as the master list of cosmic GRBs from all missions (Hurley 2010)<sup>3</sup> and the list of events recorded from soft gamma repeaters<sup>4</sup>. It turned out that four bursts from catalog 1 were known previously — these are the already mentioned GRB 070912 (Minaev et al. 2012) and three bursts recorded in the KONUS/WIND<sup>5</sup> experiment: GRB 130109, GRB 150704, and GRB 180118 (Tsvetkova et al. 2017; Frederiks et al. 2019).

<sup>2</sup>At the site [www.isdc.unige.ch/integral/science/grb#ACS](http://www.isdc.unige.ch/integral/science/grb#ACS), SPI/ACS actually has a low sensitivity for the detection of events near the IBIS pointing axis.

<sup>3</sup>The files *masterli.txt* and *cosmic1.txt* located at the site [www.ssl.berkeley.edu/ipn3](http://www.ssl.berkeley.edu/ipn3)

<sup>4</sup>The files *sgrlist.txt* and *sgrlist1.txt* located at the site [www.ssl.berkeley.edu/ipn3](http://www.ssl.berkeley.edu/ipn3)

<sup>5</sup>The site [www.ioffe.ru/LEA/kw/triggers](http://www.ioffe.ru/LEA/kw/triggers)

<sup>1</sup>At the site [www.isdc.unige.ch/integral/science/grb#ISGRI](http://www.isdc.unige.ch/integral/science/grb#ISGRI)

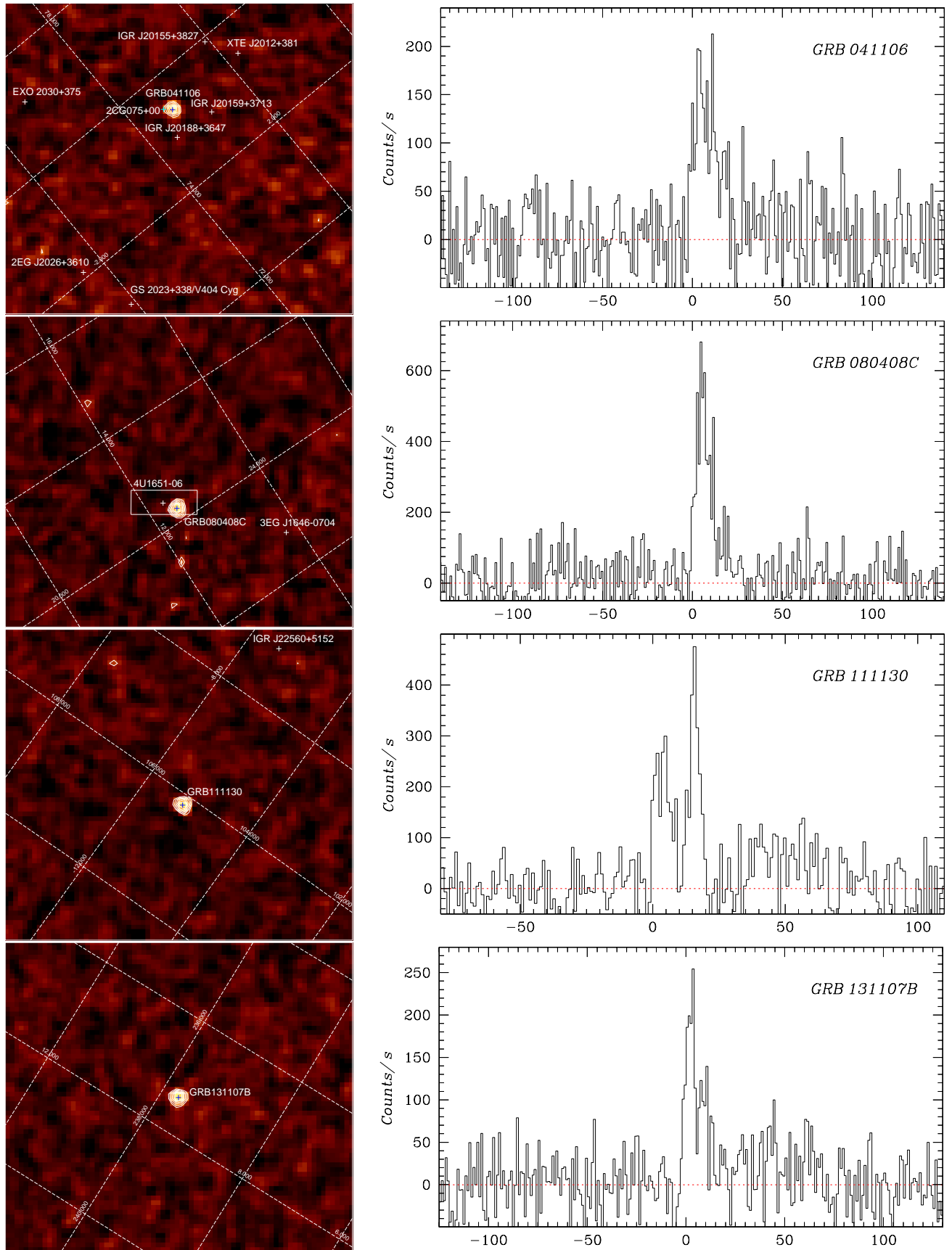


**Fig. 1.** Localization maps of GRB 041106, GRB 080408C, GRB 111130, and GRB 131107B first recorded by the IBIS/ISGRI telescope (*left*) and their time profiles in the energy range 30–100 keV (*right*).

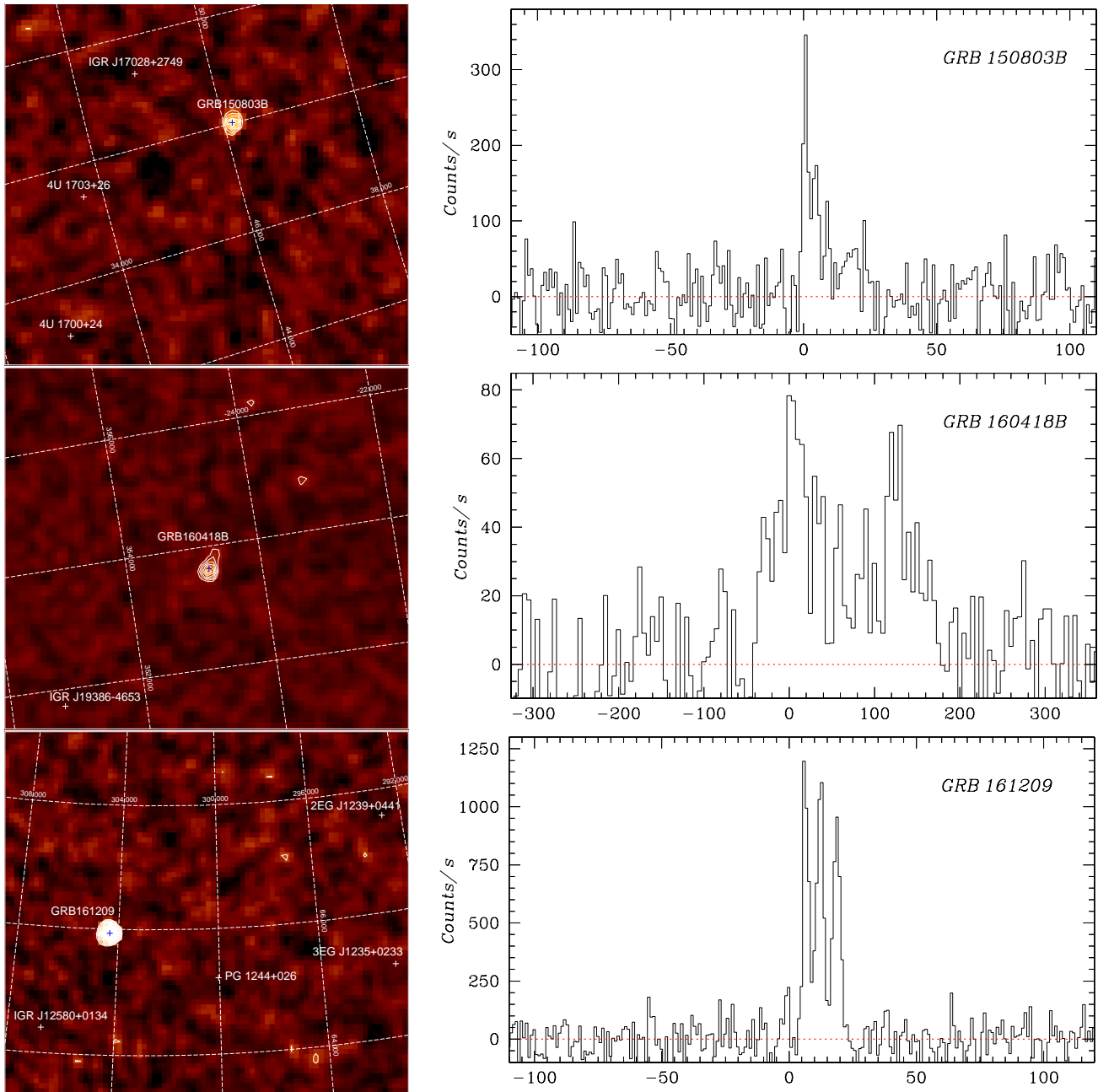


**Fig. 2.** Same as Fig. 1, but for the previously unknown GRB 150803B, GRB 160418B, and GRB 161209. The white contours in both figures indicate the levels of  $S/N = 3, 4, 5$ , etc. The positions of the known persistent emission sources in the field of view are specified.

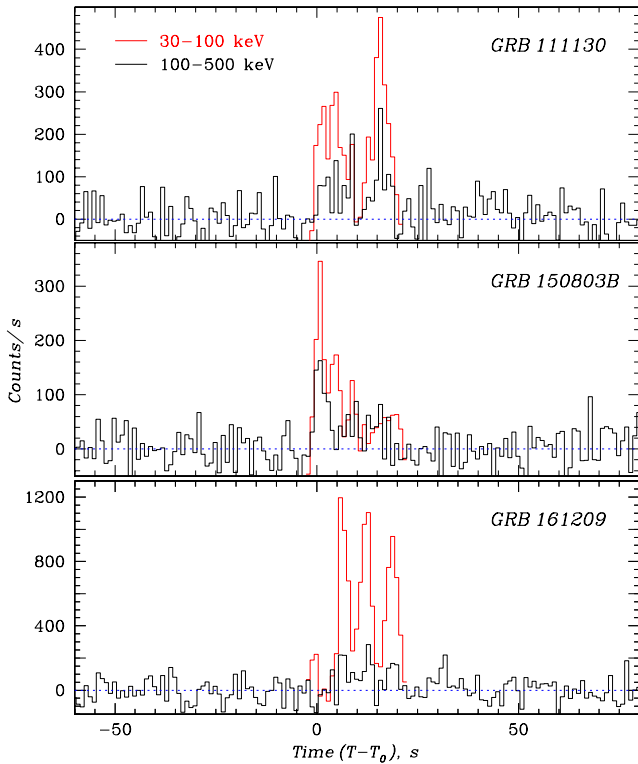


**Fig. 3.** Time profiles of GRB 111130, GRB 150803B, and GRB 161209 first recorded by the IBIS/ISGRI telescope in the energy range 100–500 keV (black histograms) and their comparison with the time profiles in the energy range 30–100 keV (red histograms).

The parameters of the remaining seven previously unknown localized GRBs from catalog 1 (GRB 041106, GRB 080408C, GRB 111130, GRB 131107B, GRB 150803B, GRB 160418B, GRB 161209) are given in Table 1. The following quantities are specified for each burst: the detection time  $T_0$ , the duration  $T_{90}$  and the duration at 10% of the peak count rate  $T_c$ , the peak count rate  $C_p$  (after background removal), the detection significance  $S/N$  from the count rate (LC) and in the image (IM), the count rate  $F$  integrated over the burst profile in the time interval  $T_{90}$  (after background removal), and the burst coordinates in the sky measured by the IBIS/ISGRI telescope. Note that  $T_c$ ,  $T_{90}$ ,  $C_p$ ,  $S/N(\text{LC})$ , and  $F$  were determined not from the detector light curve, but from the unmasked light curve obtained for the position of the burst source in the sky with allowance made for the aperture transmission.

Figures 1 and 2 present the X-ray images ( $S/N$  maps) of the sky regions within the IBIS field of view from which the bursts were localized and the burst time profiles in the energy range 30–100 keV. The contours in the images indicate the levels of  $S/N = 3, 4, 5$ , etc. The known X-ray sources are marked. We see that all of the bursts are bright; their localization, identification, and,

on the whole, reality are beyond doubt. Nevertheless, we deem them burst candidates before confirmation in the archival data of other experiments (where they might be recorded as faint events with a low confidence level and, therefore, might not enter into the basic catalogs).

Figure 3 shows the time profiles of GRB 111130, GRB 150803B, and GRB 161209 in the energy range 100–500 keV in comparison with their time profiles in the soft energy range (30–100 keV). In the hard energy range only these three bursts were recorded. For GRB 111130 and GRB 161209 this is mostly likely due to their great power; in the case of GRB 150803B this is due to (as we will see below) its anomalous hardness. On the whole, however, the hard profiles follow the soft ones, suggesting a unified single component spectrum of their emission.

This is also confirmed by Fig. 4, where the spectra of all new bursts accumulated in their interval  $T_{90}$  in the energy range 30–200 keV are presented. They are well fitted by a simple power law, as the solid lines in the figures show; only for GRB 161209 it was required to make the model more complex by introducing an exponential cutoff at high energies (dotted line). The best-fit parameters (photon index and flux) are given in Table 2. We see that out of these bursts, GRB 150803B has the hardest spectrum with  $\alpha \approx 1.06$ .

**Table 2.** Best-fit parameters for the spectra of the new GRB candidates recorded in the IBIS/ISGRI field of view

Burst (date)	$\alpha^a$	$F_X^b$
GRB 041106	$1.31 \pm 0.04$	$21.1 \pm 3.1$
GRB 080408C	$1.86 \pm 0.03$	$69.2 \pm 6.7$
GRB 111130	$1.22 \pm 0.02$	$37.6 \pm 3.4$
GRB 131107B	$1.70 \pm 0.03$	$15.8 \pm 2.0$
GRB 150803B	$1.06 \pm 0.03$	$28.7 \pm 3.7$
GRB 160418B	$2.08 \pm 0.02$	$5.5 \pm 0.4$
GRB 161209	$2.20 \pm 0.01$	$77.9 \pm 4.0$
	$1.14 \pm 0.01^c$	$68.4 \pm 3.5$

<sup>a</sup> The photon index.

<sup>b</sup> The 30–200 keV flux,  $10^{-9}$  erg  $\text{s}^{-1}$   $\text{cm}^{-2}$ .

<sup>c</sup> With the cutoff at  $E_{\text{cut}} = 46.3 \pm 2.4$  keV.

The parameters of four localized, but previously unknown bursts (missed by IBAS) analogous to those contained in Table 1 are given in Table 3. The X-ray localization maps corresponding to them and their unmasked time profiles in the energy range 30–100 keV are shown in Fig. 5. All of the bursts are powerful; after their detection by the IBIS/ISGRI telescope, they can be transferred from burst candidates, which they have deemed until now, to true GRBs. Note that with the exception of GRB 180108, all of them were detected at a statistically significant level ( $S/N \geq 9$ ) in the hard energy range 100–500 keV.

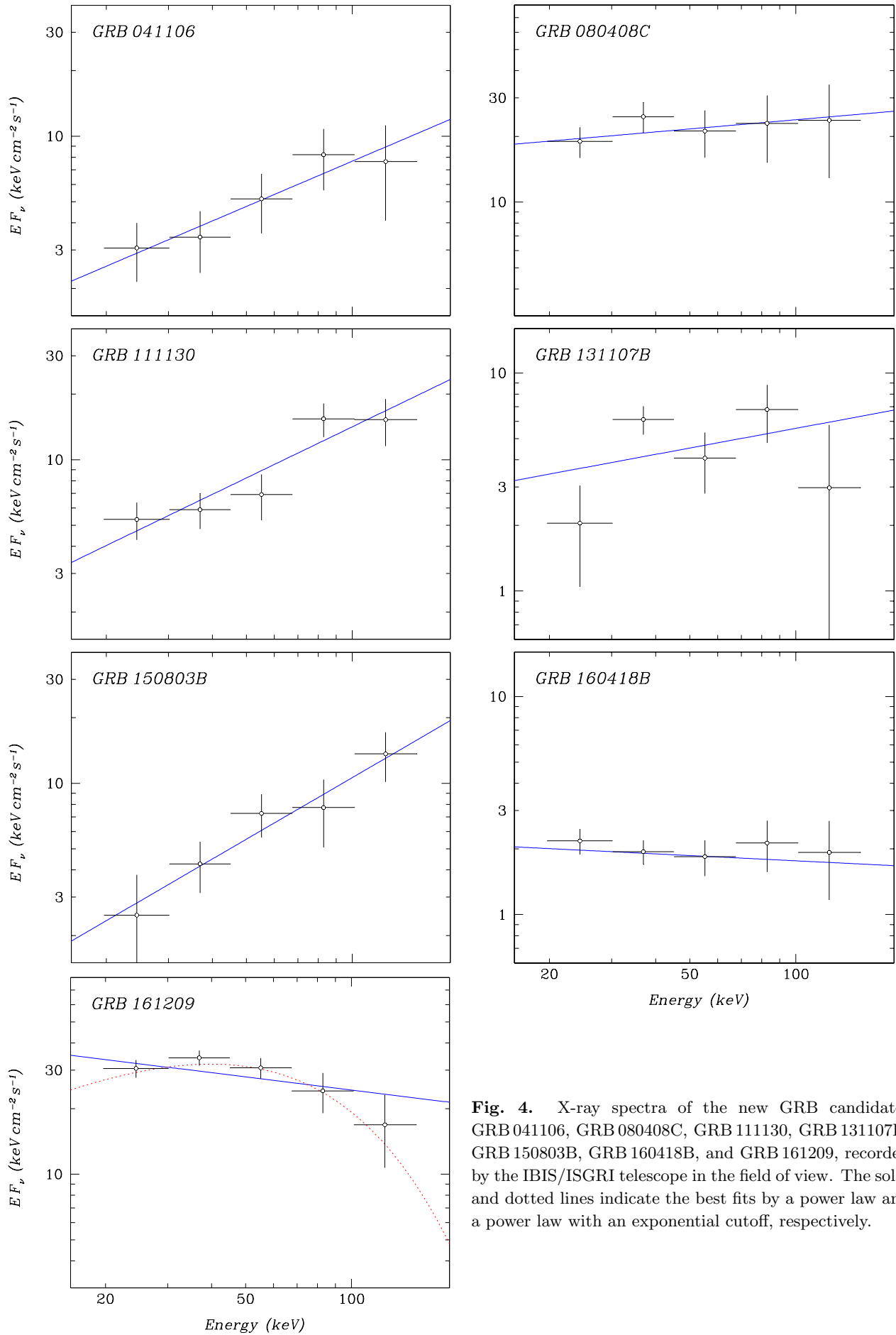


**Fig. 4.** X-ray spectra of the new GRB candidates GRB 041106, GRB 080408C, GRB 111130, GRB 131107B, GRB 150803B, GRB 160418B, and GRB 161209, recorded by the IBIS/ISGRI telescope in the field of view. The solid and dotted lines indicate the best fits by a power law and a power law with an exponential cutoff, respectively.

**Table 3.** The previously known GRBs recorded by the IBIS/ISGRI telescope of the INTEGRAL observatory within the field of view, but missed by IBAS

Burst (date)	$\Delta E^a$	$T_0^b$ (UTC)	$T_c^c$	$T_{90}^d$	$C_p^e$	$S/N^f$		$F^g$	Coordinates <sup>h</sup>		Mission <sup>i</sup>
						LC	IM		R.A.	Decl.	
						$\sigma$	$\sigma$		deg	deg	
GRB 070912	X	07:32:21	27	41	816	19	14.5	11238	264.608	-28.706	ASIJ $\underline{K}^j$
	G	07:32:21	13	36	390	10	—	3280			
GRB 130109	X	04:56:25	7	9	2787	35	19.5	9770	8.180	19.085	K
	G	04:56:25	9	17	726	9	—	2751			
GRB 150704	X	02:14:09	9	34	1231	21	14.2	6815	311.343	37.927	$\underline{K}$
	G	02:14:09	8	15	498	9	—	2126			
GRB 180108	X	10:15:37	31	52	734	11	8.4	9240	58.711	-46.267	K

<sup>a</sup> The energy range: X-ray  $X = 30\text{--}100$  keV and gamma-ray  $G = 100\text{--}500$  keV.

<sup>b</sup> The middle of the first bin with  $S/N > 3$  in the event profile on the detector light curve with a 5-s step.

<sup>c</sup> The event duration on the burst light curve at 10% of the peak count rate.

<sup>d</sup> The event duration on the burst light curve estimated by the method of Koshut et al. (1996).

<sup>e</sup> The peak count rate on the unmasked burst light curve after background removal.

<sup>f</sup> The burst detection significance from the peak count rate (LC) and in the image (IM).

<sup>g</sup> The count rate integrated over the burst profile (in the time interval  $T_{90}$ ) after background removal.

<sup>h</sup> The burst coordinates from the IBIS/ISGRI data (epoch 2000.0, a radius of the  $1\sigma$ -error circle  $\sim 1'5$ ).

<sup>i</sup> Detection in other experiments (K – KONUS/WIND, A, S, I, J – the SPI/ACS, SPI, IBIS/ISGRI, and JEM-X instruments of the INTEGRAL observatory). The underline points to an incomplete event detection by a given instrument.

<sup>j</sup> The burst was previously detected and described by Minaev et al. (2012).

The non-localized events from catalog 2 were also checked for a coincidence (within  $\pm 50$  s) with the catalogs of GRBs found in the PICsIT and SPI/ACS experiments onboard the INTEGRAL observatory and with the master list from all missions (Hurley 2010). The events that coincided with previously observed ones are listed in Table 4, whose full version is accessible at the site [hea.iki.rssi.ru/integral/ibisgrbs](http://hea.iki.rssi.ru/integral/ibisgrbs).

There are a total of 886 such events; there are an order of magnitude more events that did not coincide with any GRBs. These are mostly flares related to charged particle flux fluctuations near the Earth's magnetic poles, solar flares, and possible bursts from soft gamma repeaters and X-ray binaries. Even if there are GRBs among these events, it is impossible to identify and select them. Extrapolating the number of bursts recorded in the telescope field of view (124) to the area of the visible hemisphere of the sky (and neglecting the drop in detection efficiency for the bursts at large angles to the telescope axis), we obtain an estimate of  $\sim 2840$  for the maximum number of bursts that could be present in the sample. This number exceeds the number of actually recorded bursts by more than a factor of 3.

Out of the 39 GRBs recorded by the PICsIT detector (Bianchin et al. 2011)<sup>6</sup>, four were observed within

<sup>6</sup>Five of these 39 events are absent in the master list by Hurley (2010): GRB 060905, GRB 060928, GRB 061222A, GRB 070403, and GRB 080408B.

the IBIS field of view and were recorded by IBAS. As it turned out, all of the remaining bursts were also recorded by the IBIS/ISGRI detector and are contained in Table 4, i.e., all these events arrived laterally, from directions offset by more than  $\sim 15^\circ$  from the IBIS pointing axis<sup>7</sup>. Out of them, four events were observed only by the PICsIT detector and have now been confirmed by the ISGRI observations. Note that only 26 of the 35 PICsIT events arrived outside the field of view were recorded by the SPI/ACS detector.

If the events related to solar activity, the passage through the Earth's radiation belts, and sources of repeated bursts as well as the low-significance ( $S/N < 3$ ), short (with durations  $T_c < 1$  s) and faint (with fluxes  $C_p < 100$  counts  $s^{-1}$ ) ones are excluded from  $\sim 13500$  events recorded by SPI/ACS in the period spanned by this paper, then 1369 events, real GRB candidates, will remain. Comparing them with the 886 bursts observed by the IBIS/ISGRI detector outside the field of view, we see that IBIS/ISGRI records about 2/3 of the number of bursts recorded by the ACS detector. This is not surprising — the sensitivity of the SPI/ACS BGO detectors is, on the whole, higher than that of the IBIS/ISGRI detector (for directions outside the field of view  $\gtrsim 15^\circ$ ) and depends less on the angle to the pointing axis. The

<sup>7</sup>The IBIS field of view is a square with a side size of  $29^\circ$ , and, therefore, the bursts offset from the center by more than  $15^\circ$  can also fall into the field corners.

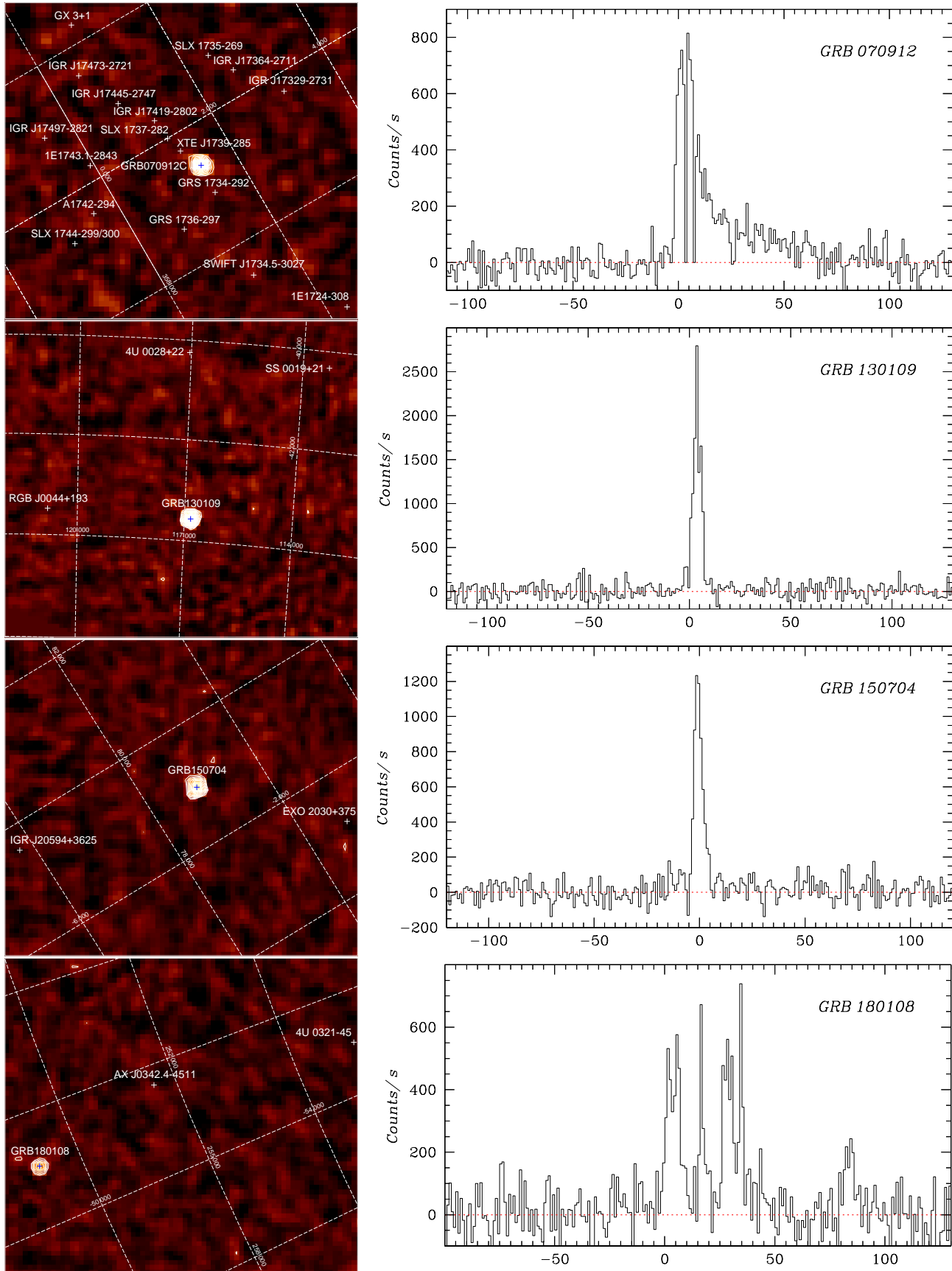


**Fig. 5.** Localization maps of GRB 070912, GRB 130109, GRB 150704, and GRB 180108 recorded by the IBIS/ISGRI telescope within the field of view (*left*) and their time profiles in the energy range 30–100 keV (*right*). The contours on the maps indicate the levels of  $S/N = 3, 4, 5$ , etc. The positions of the persistent emission sources are marked.

**Table 4.** The events recorded by the IBIS/ISGRI telescope of the INTEGRAL observatory in the detector light curves with a step  $\delta T = 5$  s at  $S/N \gtrsim 3$  coincident in time ( $\Delta T \lesssim 50$  s) with GRB candidates recorded at least by one more mission\*

Burst date	$\Delta E^a$	$T_0^b$	$\Delta T^c$	$T_c^d$	$T_{90}^e$	$C_p^f$	$S/N^g$	$F^h$	M <sup>i</sup>
		(UTC)							
		hh:mm:ss	s	s	s	counts/s	$\sigma$	counts	
2003-02-22	G	18:53:25	-32	2	10	85.3	5.1	110	A
2003-02-24	X	11:44:37	39	2	12	123.3	5.3	228	A
2003-03-19	G	23:32:54	-27	3	1	107.8	5.3	107	A
2003-05-10	X	03:32:25	0	19	71	277.3	6.1	4338	A
2003-06-09	X	23:27:40	-3	26	–	136.2	5.7	2138	A
	G	23:27:45	1	19	29	74.3	4.1	867	A
2003-07-31	X	05:14:49	17	24	27	165.6	8.0	1847	A
	G	05:14:49	17	22	29	103.7	5.9	1205	A
2003-08-11	X	21:31:31	13	116	108	142.4	7.0	4730	A
	G	21:31:36	18	89	106	90.7	5.1	2334	A
2003-08-21	X	23:24:27	7	59	72	118.6	6.2	1443	A
	G	23:25:02	42	10	46	60.1	3.3	533	A
2003-11-24	X	17:04:34	22	23	57	78.3	3.4	1444	A
2004-01-07	X	09:03:09	-4	41	47	85.0	4.4	1386	A
2004-06-21	X	18:24:47	12	15	35	150.0	7.4	1535	K
	G	18:24:47	12	15	33	160.4	8.3	1718	K
2004-08-18	X	17:31:15	-25	71	72	754.8	29.6	16567	A
	G	17:31:45	4	7	41	58.7	3.0	414	A
2004-08-23	X	13:21:03	-4	2	10	1976.3	91.9	2556	A
	G	13:21:03	-4	9	49	87.7	4.5	649	A
2004-10-05	X	13:56:48	-177	198	208	3140.6	95.8	74960	A
	G	13:59:33	-12	30	69	96.7	4.5	1226	A
2004-12-27	X	21:28:04	3	2	7	1514.6	50.5	1591	A
2004-12-30	X	06:26:04	5	23	–	129.7	6.2	990	A
	G	06:26:04	5	16	8	61.4	3.2	223	A
2005-02-23	X	09:34:29	3	7	–	119.9	4.7	454	H
2005-02-28	X	22:28:06	-4	18	28	390.6	16.6	1992	A
2005-04-04	X	21:34:36	-38	121	123	783.4	9.1	16329	A
2005-08-11	X	13:35:48	2	2	8	466.7	22.4	499	A
2006-03-19	X	00:24:52	11	37	30	137.5	4.2	1799	A
2006-09-05	X	14:47:05	-105	240	217	1131.8	38.4	118243	P
	G	14:47:35	-75	96	157	495.8	19.5	22536	P
2006-09-11	X	08:56:44	2	2	31	148.7	6.5	437	A
2006-09-16	X	23:42:55	1	2	2	2055.6	88.9	2754	A
2006-09-28	X	01:19:59	15	26	35	645.4	29.2	7712	AP
	G	01:19:47	3	25	29	811.4	37.0	10984	AP
2006-12-22	G	03:30:12	-2	5	18	173.1	7.8	905	P
2006-12-24	X	15:38:12	5	62	57	135.5	5.2	3930	A
	G	15:38:42	35	7	25	62.8	2.9	461	A
2006-12-24	X	18:43:09	1	42	78	98.5	3.9	3660	A
	G	18:43:39	31	4	27	58.9	2.5	448	A
2006-12-24	X	19:56:21	-9	56	59	125.7	4.8	3741	A
	G	19:56:31	0	7	37	89.7	4.1	760	A
2006-12-24	X	21:58:45	4	42	44	615.8	26.4	13949	A
	G	21:59:05	24	27	36	161.9	7.0	2496	A
2006-12-25	X	00:47:04	9	10	14	228.4	9.7	702	A
2007-01-17	X	00:28:11	3	38	29	246.8	10.6	3694	A
	G	00:28:11	3	25	27	79.8	3.6	955	A
2007-01-29	G	22:47:19	35	2	–	107.3	4.8	130	Z
2007-01-31	X	02:13:18	7	47	101	169.0	4.0	4980	A

\* The full version of the table is accessible at the site [hea.iki.rssi.ru/integral/ibisgrbs](http://hea.iki.rssi.ru/integral/ibisgrbs)

**Table 4.** (Contd.)

Burst date	$\Delta E^a$	$T_0^b$	$\Delta T^c$	$T_c^d$	$T_{90}^e$	$C_p^f$	$S/N^g$	$F^h$	$M^i$
		(UTC)							
		hh:mm:ss	s	s	s	counts/s	$\sigma$	counts	
2007-04-03	X	12:40:17	-10	48	54	906.0	29.4	26207	P
	G	12:40:22	-5	49	54	313.5	13.4	8768	P
2007-04-07	X	14:24:24	1	2	8	182.6	7.7	211	Z
2007-09-18	X	17:08:47	0	3	26	499.3	21.9	790	A
2007-11-20	X	11:40:02	1	24	49	113.8	5.0	1620	A
	G	11:40:07	6	10	19	57.0	2.5	411	A
2007-11-24	X	15:07:46	6	21	–	74.6	2.4	437	A
2007-11-24	X	17:26:17	35	6	26	98.6	4.2	808	A
2008-01-08	X	08:33:16	32	29	87	328.5	9.8	4784	A
	G	08:32:51	7	51	102	135.3	5.4	3063	A
2008-01-08	X	23:27:01	-6	53	54	271.0	10.6	7055	A
	G	23:27:06	-1	33	38	105.8	4.5	1988	A
2008-02-03	X	04:54:51	4	18	31	150.6	6.4	1749	A
	G	04:54:51	4	3	12	90.8	3.9	270	A
2008-02-03	X	11:03:20	-6	14	24	94.7	3.8	1037	A
	G	11:03:25	-1	8	53	83.3	3.5	815	A
2008-02-12	X	17:15:33	-28	55	57	187.9	7.5	4098	A
	G	17:16:18	16	8	40	50.9	2.3	442	A
2008-02-14	X	20:14:42	0	61	50	264.9	6.9	7335	A
	G	20:15:02	19	21	32	83.8	3.4	884	A
2008-02-14	X	20:29:24	1	21	43	175.5	6.3	2464	A
2008-02-29	X	22:04:16	5	6	22	229.3	5.6	1803	A
2008-02-29	X	22:24:41	3	87	75	366.6	13.2	12830	A
	G	22:25:21	43	19	38	106.1	4.5	1292	A
2008-02-29	X	22:44:36	0	101	119	182.9	6.6	7850	A
	G	22:44:46	10	12	44	76.5	3.3	1086	A
2008-03-01	X	00:43:26	-2	57	93	352.0	13.7	5339	A
2008-03-01	X	04:22:43	26	56	49	214.3	8.6	5479	A
	G	04:22:43	26	58	100	86.6	3.7	2345	A
2008-03-02	X	06:51:09	2	31	35	143.7	5.3	1679	A
	G	06:51:09	2	3	40	69.4	2.9	753	A
2008-03-08	X	12:04:47	-5	43	36	173.6	6.1	3203	A
	G	12:04:57	4	44	33	128.3	4.9	2438	A
2008-03-13	X	11:03:37	6	69	85	159.2	6.0	3882	A
	G	11:04:12	41	40	44	100.1	4.3	1613	A
2008-03-13	X	13:36:56	9	79	68	395.4	9.7	12137	A
	G	13:36:56	9	18	16	99.3	4.2	920	A
2008-03-13	X	13:39:56	-10	97	19	242.5	6.0	2324	A
	G	13:40:01	-5	10	21	74.8	3.2	375	A
2008-03-13	X	13:43:06	-1	98	80	232.7	5.7	8334	A
	G	13:43:16	8	15	45	70.7	3.0	789	A
2008-03-27	X	19:24:58	0	12	30	110.6	4.2	1075	A
	G	19:25:03	4	9	–	70.3	3.0	418	A
2008-04-08	X	10:21:34	-110	119	116	1404.7	31.0	37709	P
	G	10:21:39	-105	121	125	241.6	8.3	9027	P
2008-04-14	X	15:40:02	-7	2	5	141.7	6.3	196	A
2008-05-05	X	14:41:27	-8	17	22	222.5	8.9	2006	A
2008-10-11	X	17:39:12	-50	78	72	207.9	7.0	3247	A
2008-10-31	X	01:48:30	11	65	60	194.5	5.7	6129	A
	G	01:48:30	11	51	53	90.8	3.7	2036	A
2008-11-08	X	13:00:25	20	36	63	183.4	4.9	4775	A

Table 4. (Contd.)

Burst date	$\Delta E^a$	$T_0^b$	$\Delta T^c$	$T_c^d$	$T_{90}^e$	$C_p^f$	$S/N^g$	$F^h$	$M^i$
		(UTC)							
		hh:mm:ss	s	s	s	counts/s	$\sigma$	counts	
2009-01-03	X	12:23:27	-36	58	81	155.5	6.1	5065	A
	G	12:24:32	28	10	51	90.2	3.9	834	A
2009-04-01	X	00:03:03	23	9	9	101.2	4.1	335	A
	G	00:03:03	23	4	21	124.2	4.9	307	A
2010-02-26	G	04:46:15	-1	4	4	102.3	4.2	202	A
2010-08-10	G	00:51:21	16	1	1	163.3	7.0	163	Z
2010-10-14	X	04:15:19	9	10	22	347.7	14.0	1285	A
	G	04:15:14	4	6	37	194.3	8.0	569	A
2011-03-02	G	16:27:00	47	19	–	79.9	3.3	923	A
2011-09-03	X	02:42:31	-15	38	37	442.5	18.2	9107	A
	G	02:42:31	-15	25	42	290.1	12.2	4158	A
2011-09-08	X	15:42:51	-15	36	48	228.4	9.5	4036	A
	G	15:43:06	0	17	42	96.2	4.1	1729	A
2011-09-26	X	20:16:59	6	54	53	386.8	14.3	11582	A
2011-12-05	X	15:17:05	4	17	15	65.7	3.1	344	K
2011-12-28	X	15:45:33	0	6	23	105.4	4.8	484	A
2012-02-14	X	19:07:36	9	2	–	126.7	5.4	146	S
2012-06-03	X	17:53:18	5	26	47	406.9	3.8	5871	A
	G	17:53:18	5	19	42	107.7	3.5	1277	A
2012-06-24	X	22:24:02	3	16	28	162.2	7.2	899	A
	G	22:24:02	3	13	10	130.1	5.7	457	A
2012-06-28	X	16:10:57	-3	72	69	355.4	16.1	5432	A
	G	16:11:02	1	7	26	84.6	3.9	722	A
2012-07-06	X	23:04:49	0	146	253	2299.7	84.8	176156	A
	G	23:04:59	10	139	154	1952.8	75.8	138736	A
2012-08-02	X	13:41:54	8	19	68	140.3	5.0	2491	A
	G	13:41:54	8	15	55	129.3	5.1	1509	A
2012-09-16	X	04:07:47	2	5	13	99.2	3.7	393	A
2012-11-27	X	15:55:33	-23	27	33	207.0	10.2	2623	A
	G	15:55:53	-3	28	44	143.0	6.8	2391	A
2013-02-19	X	18:37:12	3	10	22	135.2	4.6	747	A
	G	18:37:12	3	9	23	143.2	4.2	960	A
2013-03-20	X	13:24:08	1	13	12	192.2	8.9	1183	A
	G	13:24:08	1	5	9	242.9	11.8	831	A
2013-06-23	X	07:01:36	-2	41	37	572.1	28.7	7876	A
2013-09-07	X	21:39:21	3	19	15	181.9	9.1	1217	A
	G	21:39:21	3	16	14	134.4	6.0	808	A
2014-04-13	X	11:27:27	-9	11	10	253.6	11.8	1272	Z
2014-10-16	X	13:01:16	-24	41	41	520.8	20.9	9339	A
	G	13:01:26	-14	26	30	286.7	12.8	3846	A
2014-10-29	X	03:14:34	-23	10	34	110.4	5.9	768	A
	G	03:14:39	-18	5	21	86.3	4.1	261	A
2014-12-31	X	15:09:22	0	78	78	163.6	6.7	4569	A
	G	15:09:27	5	58	73	74.3	3.4	1817	A
2015-02-06	X	14:31:25	13	24	38	115.7	6.1	1413	A
	G	14:31:20	8	25	44	200.8	9.9	1572	A
2015-03-09	X	23:00:04	19	20	17	125.1	5.5	1141	A
	G	22:59:59	14	20	22	206.8	9.9	1988	A
2015-03-30	X	19:54:07	-17	27	31	430.2	22.5	4077	A
	G	19:54:07	-17	26	42	770.3	35.6	6094	A

**Table 4.** (Contd.)

Burst date	$\Delta E^a$	$T_0^b$	$\Delta T^c$	$T_c^d$	$T_{90}^e$	$C_p^f$	$S/N^g$	$F^h$	$M^i$
		(UTC)							
		hh:mm:ss	s	s	s	counts/s	$\sigma$	counts	
2015-07-04	X	02:14:11	0	9	11	177.8	8.7	653	K
	G	02:14:11	0	8	9	113.8	5.5	426	K
2015-12-29	X	03:01:05	-14	63	65	300.4	11.9	11068	K
	G	03:01:15	-4	56	56	141.7	5.8	3554	K
2016-02-15	X	18:36:23	0	12	32	85.3	3.8	1157	A
	G	18:36:23	0	21	21	153.6	6.5	1164	A
2016-08-06	G	09:30:42	7	68	88	83.7	3.4	2013	A
2016-08-21	X	20:36:26	5	36	39	559.6	25.5	9500	A
	G	20:36:26	5	40	37	660.7	27.5	10899	A
2016-09-20	X	07:26:32	0	17	17	335.8	15.6	3074	A
2016-10-18	X	00:58:58	4	63	46	632.6	24.4	7880	A
	G	00:58:58	4	63	60	555.3	21.1	7221	A
2016-12-23	X	20:59:11	-1	33	31	125.5	6.0	1586	A
	G	20:59:26	13	21	39	88.8	3.7	1117	A
2016-12-26	X	03:15:50	3	3	–	224.1	11.0	370	A
2017-02-18	X	17:58:10	-2	23	70	361.1	13.7	4232	A
	G	17:58:10	-2	19	–	138.4	5.2	1274	A
2017-05-20	X	15:30:29	5	4	2	106.5	4.9	106	A
	G	15:30:29	5	3	12	196.5	7.8	583	A
2017-06-01	X	08:27:41	0	52	9	113.1	5.0	286	A
	G	08:27:46	4	7	41	87.2	3.4	464	A
2017-08-19	X	02:38:49	-13	24	20	486.7	24.0	4677	A
2017-11-10	X	08:40:17	-1	27	35	133.4	6.2	2014	A
2018-01-08	X	10:15:37	3	34	93	123.6	5.5	1889	K

<sup>a</sup> The energy range:  $X = 30\text{--}100$  keV and  $G = 100\text{--}500$  keV.

<sup>b</sup> The middle of the first bin with  $S/N > 3$  in the event profile on the detector light curve with a 5-s step.

<sup>c</sup> The delay relative to the closest known burst (a negative value means that the IBIS/ISGRI telescope saw the event earlier).

<sup>d</sup> The duration on the detector light curve at 10% of the peak count rate.

<sup>e</sup> The duration on the detector light curve using the method of Koshut et al. (1996).

<sup>f</sup> The peak count rate on the detector light curve with a 1-s step (the background was removed).

<sup>g</sup> The burst detection significance from the peak count rate.

<sup>h</sup> The count rate integrated over the burst profile with a 1-s step (in the time interval  $T_{90}$  after background removal (if  $T_{90}$  was not determined, then  $T_c$  is used)).

<sup>i</sup> The mission in which a given burst was previously recorded (as a rule within  $\pm 50$  s): A, P – INTEGRAL SPI/ACS and IBIS/PICsIT, H – HETE, K – KONUS/WIND, S – SWIFT/BAT, Z – SUZAKU.

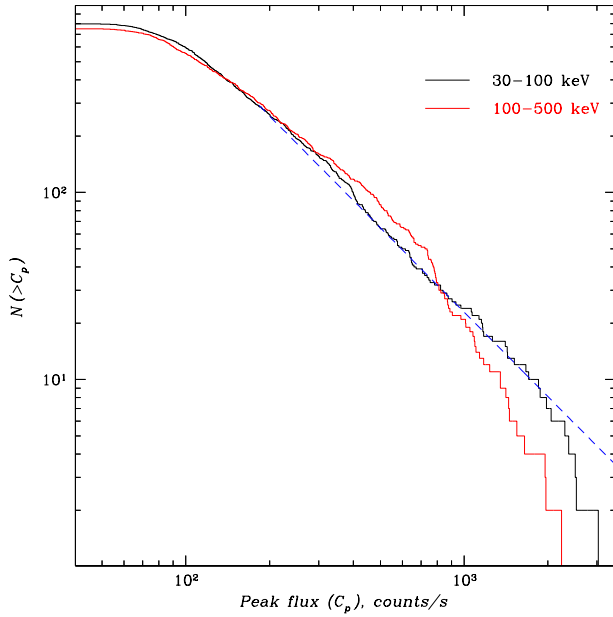


**Fig. 6.** Distribution of the number of bursts recorded by the IBIS/ISGRI telescope with a peak flux above a certain value  $C_p$  (in counts/s) as a function of  $C_p$ . The black and red solid histograms indicate the distributions of the bursts recorded in the energy ranges 30–100 and 100–500 keV; the dashed line indicates the power law with an exponent of  $3/2$  expected for a uniform distribution of the burst sources.

maximum sensitivity ranges of the detectors differ noticeably: 20–200 keV for IBIS/ISGRI and  $\gtrsim 75$  keV for SPI/ACS, which also affects the ratio of the numbers of recorded bursts. Clearly, SPI/ACS is more efficient in detecting hard bursts.

Curiously, Table 4 actually contains only 787 bursts observed by the SPI/ACS detector, i.e., SPI/ACS did not see nearly 100 bursts of those recorded by the IBIS/ISGRI detector. This may be a consequence of an appreciable number of soft bursts to which SPI/ACS is weakly sensitive, but to which IBIS/ISGRI is sensitive. Note that 59 SPI/ACS bursts that were also recorded by the IBIS/ISGRI detector are absent in the master list by Hurley (2010).

The existence of bursts recorded by IBIS/ISGRI, but missed by SPI/ACS is clearly seen, in particular, from the abridged version of Table 4 directly included in the paper. Only 110 GRBs for which there is also a confirmation only in one experiment, apart from the detection by the IBIS/ISGRI telescope (both SPI/ACS and IBIS/PICsIT saw GRB 060928, but these are detectors of one mission), were left in it. The table contains 15 bursts that were not recorded by the SPI/ACS detector. The detection of these bursts by IBIS/ISGRI allows all of the bursts in this table to be transferred from candidates, which they have been deemed until now, to real bursts. Table 4 (just as its main version) gives the follow-

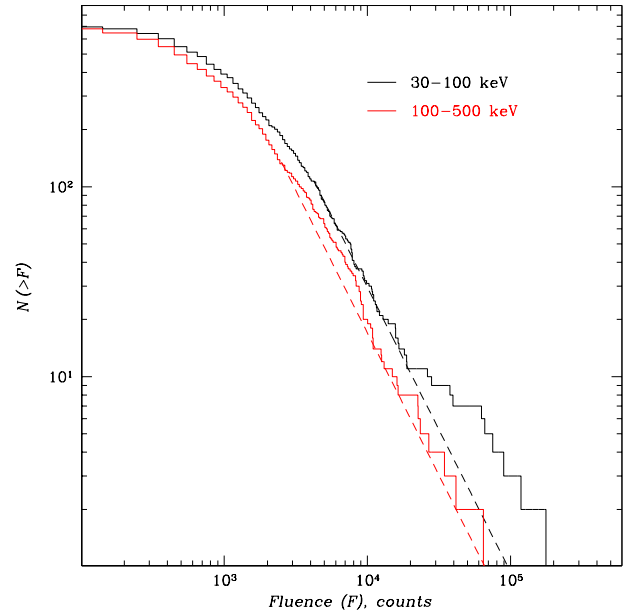


**Fig. 7.** Distribution of the number of bursts recorded by the IBIS/ISGRI telescope with a fluence above a certain value  $F$  (in counts) as a function of  $F$ . The black and red solid histograms indicate the dependences for the bursts recorded in the energy ranges 30–100 and 100–500 keV. The dashed lines indicate the corresponding power laws with an exponent of  $3/2$  expected for a uniform distribution of the burst sources.

ing parameters: the detection time  $T_0$ , the delay relative to the closest known burst  $\Delta T$ , the duration  $T_{90}$  and the duration at 10% of the peak count rate  $T_c$ , the peak count rate  $C_p$  (after background removal), the detection significance  $S/N$  from the count rate, the count rate  $F$  integrated over the burst profile in the time interval  $T_{90}$  (after background removal), and the missions that observed a burst previously (A, P – INTEGRAL SPI/ACS and IBIS/PICsIT, H – HETE, K – KONUS/WIND, S – SWIFT/BAT, Z – SUZAKU). In contrast to Tables 1 and 3, these parameters were determined from the detector light curve, without taking into account the real efficiency of the GRB observation.

## DISCUSSION

The sample of IBIS/ISGRI bursts found in this paper and recorded by IBAS is quite representative ( $7 + 4 + 886 + 113 = 1010$  events) and can be used to obtain some statistical dependences. For example, Fig. 6 presents the distribution of the number of IBIS/ISGRI bursts with a peak flux above a certain value  $C_p$  as a function of  $C_p$ , while Fig. 7 presents the distribution of the number of bursts with a fluence above  $F$  as a function of  $F$ . We see that the  $C_p$  distribution of the hard bursts recorded in the energy range 100–500 keV differs noticeably from the uniform one  $\sim C_p^{-3/2}$ . The distribution of the soft

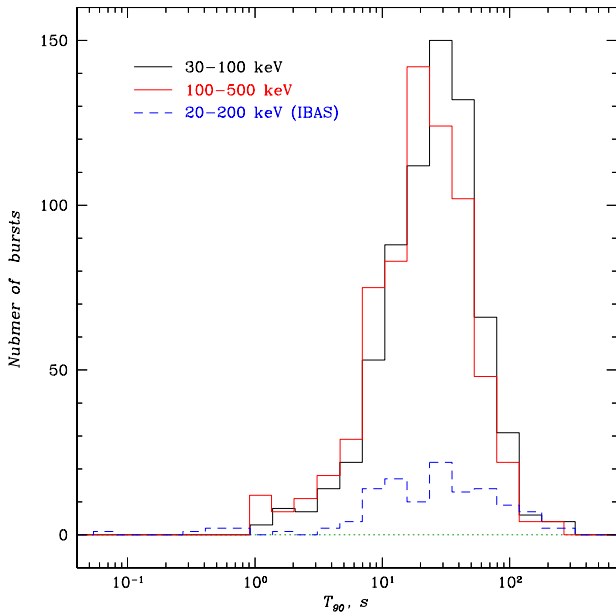


**Fig. 8.** Distribution of the bursts recorded by IBIS/ISGRI in their duration  $T_{90}$  (the black and red histograms represent the bursts in the energy ranges 30–100 and 100–500 keV, respectively; the blue dashed histogram represents the bursts recorded by IBAS in the energy range 20–200 keV).

bursts recorded in the energy range 30–100 keV virtually follows the uniform one. Note also a clear excess of soft bursts with a large fluence  $F$  above the hard bursts. There is no such clear excess in the distribution of the bursts in peak flux. Therefore, the bursts responsible for the excess apparently have a longer duration.

Figure 8 shows the distribution of the number of bursts in duration  $T_{90}$  as a function of the energy range. The blue dashed line separately indicates the distribution of the bursts recorded by IBAS in the telescope’s field of view. The mean duration is  $\sim 18$  s. At the same time, we see that the bursts arrived outside the IBIS field of view are, on the whole, shorter than those recorded in the field of view (by IBAS). The bursts recorded in the hard energy range are shorter than those recorded in the soft one. Such a decrease in the duration of both the individual pulses in the burst time profile and the entire burst with increasing lower threshold of the energy range were also observed in earlier experiments (Fenimore et al. 1995; Minaev et al. 2010b).

In Fig. 9 the burst hardness (the ratio of the fluences in the energy ranges 100–500 and 30–100 keV) is shown as a function of burst duration  $T_{90}$ . Naturally, only those bursts that were recorded in both soft and hard energy ranges are presented here. The red asterisks mark the bursts from Table 1 discovered in our work; the blue crosses mark the localized bursts missed by IBAS from Table 3. On the whole, the distribution has a fairly symmetric shape. This is primarily because there are no

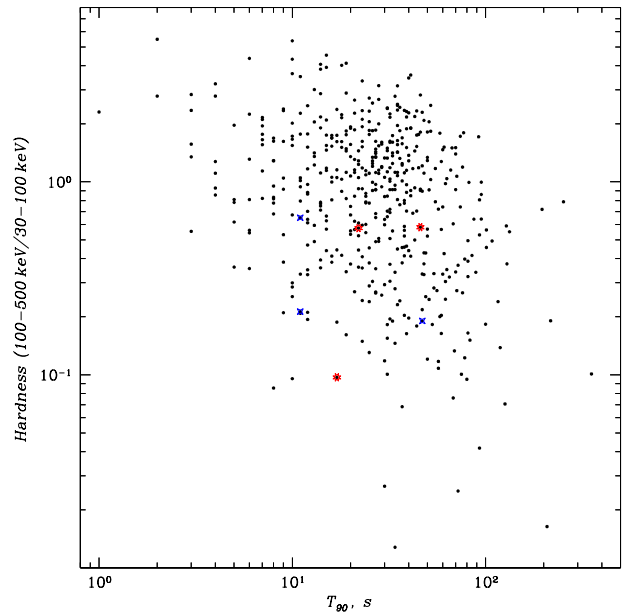


**Fig. 9.** Correlation between the hardness of the IBIS/ISGRI bursts (the ratio of the fluences in the energy ranges 100–500 and 30–100 keV) and their duration  $T_{90}$  (black dots). If the time  $T_{90}$  was not determined, then  $T_c$  is used. The red and blue asterisks mark the bursts discovered in this paper and the localized bursts missed by IBAS, respectively.

short events in the sample excluded due to the burst search method used. For this reason, there is no the well-known cluster of short hard bursts in the figure. Note also that some bursts deviate greatly from the general distribution, in particular, very soft bursts whose hardness differs from the mean for the sample by an order of magnitude or more.

Finally, Fig. 10 presents the distribution of the time interval between bursts recorded by IBIS/ISGRI. The most probable time between bursts  $\Delta T \simeq 4.2$  days is indicated by the dashed line. The distribution is highly asymmetric. In the region of short time intervals it reaches  $\sim 900$  s. Bursts with a precursor (see, e.g., Lazzati 2005; Minaev and Pozanenko 2017), bursts with extended emission (see, e.g., Burenin et al. 1999; Gehrels et al. 2006; Minaev et al. 2010a; Barkov and Pozanenko 2011), and ultra-long bursts (see, e.g., Gendre et al. 2013) can fall here. In the region from a few to ten hours the distribution can be slightly distorted due to the sampling interval of the INTEGRAL observations, in particular, due to the times related to the passage through the orbital perigee and the Earth’s radiation belts, when all instruments are switched off. On long time intervals the number of recorded bursts drops rapidly.

The presented distributions may be distorted to some extent by the IBIS/ISGRI detector shield, because the bursts that arrived at large angles to the IBIS axis

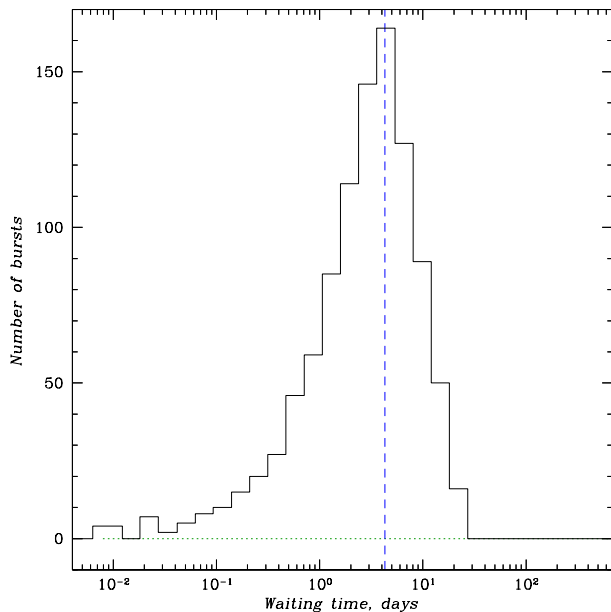


**Fig. 10.** Distribution of the time interval between IBIS/ISGRI bursts. The most probable time between bursts  $\Delta T \simeq 4.2$  days is indicated by the dashed line.

and did not fall within its field of view constitute the bulk of the bursts in the sample. We can understand that this distortion is significant by comparing the flux from bursts measured by the ISGRI detector with the flux measured from them in other experiments. The results of such a study performed for a subsample of bursts recorded simultaneously by the IBIS/ISGRI and FERMI/GBM instruments are presented in the Appendix to this paper.

Measuring the IBIS/ISGRI detection efficiency of GRBs arrived at large angles to the IBIS axis is important primarily for problems related to the search for and investigation of bursts associated with LIGO/Virgo gravitational-wave events in the IBIS/ISGRI data. For example, GRB 170817A recorded by the FERMI/GBM monitor (Goldstein et al. 2017) and identified with the first such event GW 170817 associated with the merger of a neutron star binary system (Abbott et al. 2017) consisted of two episodes: the first, short and rather hard one, and the second, considerably softer one (Pozanenko et al. 2018). The first event was recorded by the SPI/ACS detector, which is sensitive at energies  $\gtrsim 75$  keV, while the second one was not (Savchenko et al. 2017).

For a favorable combination of circumstances the IBIS/ISGRI telescope is able to record the soft component of such bursts simultaneously with the detection of the hard component by SPI/ACS. The FERMI/GBM experiment, which is close in sensitivity and energy range, by no means always can observe such a burst due to the low satellite orbit and the high probability of its

shadowing by the Earth. There was such a situation (for more details, see Pozanenko et al. 2019) when the second gravitational-wave event S190425z from the merger of a pair of neutron stars was recorded in the LIGO/Virgo experiment (Singer 2019). During this event the SPI/ACS detector onboard the INTEGRAL observatory recorded a significant excess of the count rate (Martin-Carillo et al. 2019; Minaev et al. 2019), while the GBM monitor onboard the FERMI observatory did not (Fletcher 2019).

## CONCLUSIONS

We searched for GRBs and other hard X-ray transient events in the archival data from the IBIS/ISGRI telescope of the INTEGRAL observatory obtained during the observations from February 2003 to January 2018; the useful operation time of the telescope over this period was 405 Ms. Seven previously unknown bursts missed by IBAS were recorded in the IBIS field of view. The bursts were localized with an accuracy better than 2 arcmin. Four more bursts missed by IBAS, but found previously by other INTEGRAL telescopes or other missions were also recorded in the field of view. Thus, 11 bursts were detected and localized in the field of view, which account for 10% of the number of bursts detected by IBAS. For GRB 161209 we were able to determine the characteristic energy  $E_c \simeq 46$  keV of the spectral cutoff needed to place the event on the  $E_p - E_{\text{iso}}$  correlation diagram (Amati 2002). It seems of paramount importance to check the coincidence of the well-localized bursts found with the list of supernovae observed at this time.

A large number (886) of GRBs previously detected in other experiments were recorded outside the IBIS field of view. These are the bursts that passed outside the coding mask through the gap between the mask and detector. Those events that before our search in the IBIS/ISGRI data were recorded only by one instrument (mostly by the ACS of the SPI gamma-ray spectrometer onboard the INTEGRAL observatory) from the burst candidates can, thus, be transferred to true cosmic bursts. We compiled the catalogs of recorded bursts into which their basic parameters were introduced. The correlations between the parameters of the bursts found were investigated.

We investigated the detection efficiency of bursts at various energies as a function of the angle between the burst arrival direction and the IBIS pointing axis. We obtained the calibration function, which can be used to estimate the hard X-ray fluxes from GRBs and gravitational-wave events occurring at large angular distances from the center of the field of view.

The total number of hard short events recorded by the IBIS/ISGRI telescope exceeds the number of events included in the catalog of bursts by one order of magnitude or more. Undoubtedly, there are GRBs among

them, but it is impossible to separate them from solar flares, magnetospheric events, events related to charged particle flux fluctuations in the spacecraft orbit and detector activation by cosmic-ray particles. *The very fact of the detection of such a large number of GRBs that did not arrive from the field of view shows that the capabilities of the IBIS/ISGRI telescope for investigating GRBs were greatly underestimated. It is necessary to carry out a continuous monitoring of transient events in the newly incoming INTEGRAL data and to compare the events found with those recorded by the SPI/ACS detector and any other missions.* The IBIS/ISGRI telescope allows the X-ray and gamma-ray spectrum of the recorded GRBs to be measured and, therefore, can become an important supplement to the SPI/ACS detector, which provides no spectral information. Moreover, as shown in this paper, the telescope records a certain number (10–15%) of bursts not triggered in SPI/ACS.

#### ACKNOWLEDGMENTS

This work is based on the long-term observations performed by the INTEGRAL international astrophysical gamma-ray observatory and retrieved via the Russian and European INTEGRAL Science Data Centers.

#### FUNDING

We are grateful to the Russian Science Foundation for financial support of this study (project no. 18-12-00522).

#### APPENDIX

##### CALIBRATION OF THE OBSERVATIONS OF BURSTS OUTSIDE THE FIELD OF VIEW

To determine the sensitivity of the IBIS/ISGRI telescope to the observation of GRBs at large angles to its pointing axis, we compiled a sample of bursts recorded simultaneously by the IBIS/ISGRI telescope and the FERMI/GBM<sup>8</sup> monitor (Bhat et al. 2016). The bursts recorded by IBIS/ISGRI within its field of view (from Tables 1 and 3 and the list of bursts revealed by IBAS, see [www.isdc.unige.ch/integral/science/grb#ISGRI](http://www.isdc.unige.ch/integral/science/grb#ISGRI)) were added to the IBIS/ISGRI bursts from Table 4. The sample included 306 events; the events were deemed coincident if their arrival times in these two instruments differed by no more than  $2 \times T_{90}$ , where the event duration  $T_{90}$  was taken from the FERMI/GBM burst catalog.

For each burst we determined the ratio  $K$  of the fluence in the energy range 10 keV – 1 MeV in units of [erg cm<sup>-2</sup>] measured by the FERMI/GBM monitor to

<sup>8</sup>[heasarc.gsfc.nasa.gov/W3Browse/fermi/fermigbrst.html](http://heasarc.gsfc.nasa.gov/W3Browse/fermi/fermigbrst.html)

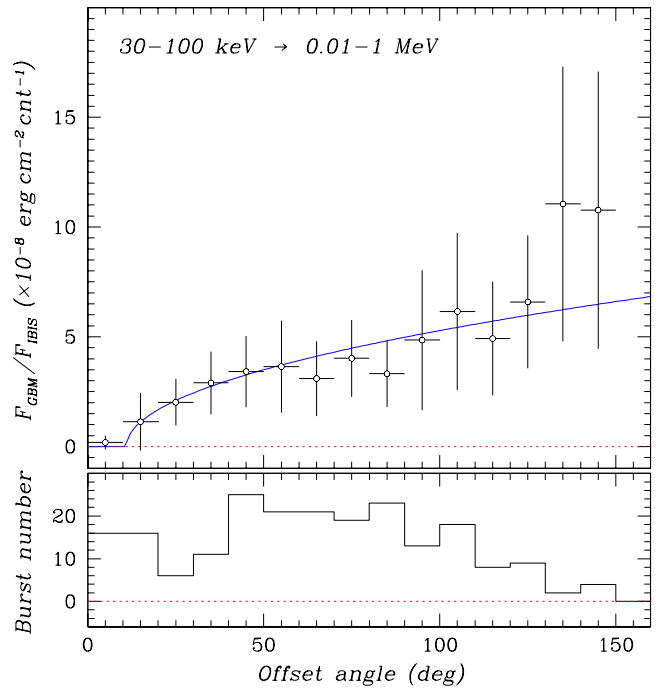


**Fig. 11.** Conversion factor from the GRB fluence recorded (in counts) by the IBIS/ISGRI detector in the energy range 30–100 keV to the fluence of the FERMI/GBM monitor in the energy range 10–1000 keV versus angle between the burst direction and the IBIS pointing axis.

its fluence in [counts] measured by the IBIS/ISGRI detector (see Table 4). Figures 11 and 12 show this ratio as a function of the angle  $\theta$  (with a  $10^\circ$  step) between the GRB direction (according to the FERMI/GBM localization) and the IBIS axis, respectively, for the two IBIS/ISGRI detector energy ranges 30–100 and 100–500 keV used. The errors of the values in each bin in angle are the root-mean-square ones for the events in this bin. The distribution of the number of events (bursts) in the bins is presented on the lower panels of the figures. We see that more than 40–50 bursts observed within the IBIS/ISGRI field of view were also recorded by the FERMI/GBM monitor. The presented dependences describe well the drop in the telescope’s sensitivity to the detection of GRBs up to angles  $\theta \sim 100^\circ$  to the IBIS axis. Clearly, the dependences cannot not be used for the bursts within the IBIS/ISGRI field of view (at an angular distance from the axis  $\lesssim 15^\circ$ ). The fluxes for such bursts can be determined much more accurately using the response matrix of the telescope itself.

For the convenience of estimates, the dependences of the factor  $K = F_{\text{GBM}}/F_{\text{IBIS}}$  on angle  $\theta$  presented in the figures were fitted by simple expressions,  $K_s = 5.6 \times 10^{-9} \sqrt{\theta - 11^\circ} \text{ erg cm}^{-2} \text{ count}^{-1}$  and  $K_h = 3.3 \times 10^{-9} \sqrt{\theta - 11^\circ} \text{ erg cm}^{-2} \text{ count}^{-1}$  for the ranges 30–100 keV and 100–500 keV, respectively. These analytical dependences are indicated in the figures by the solid

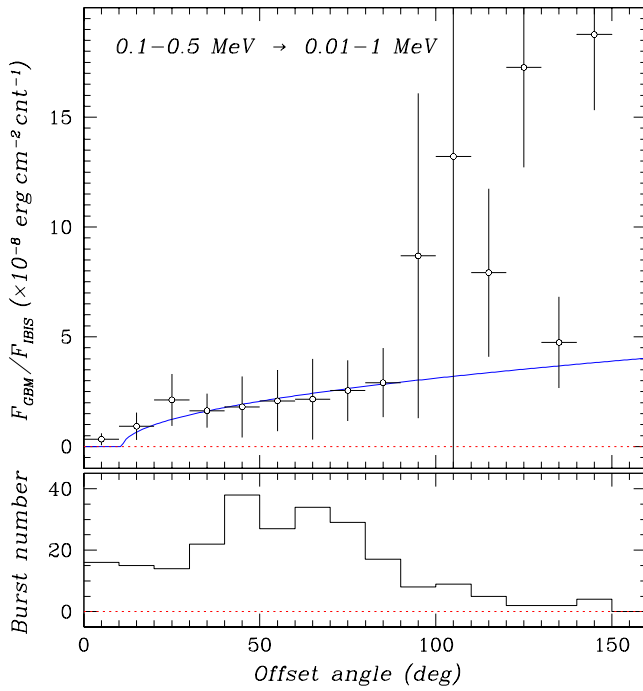


**Fig. 12.** Same as Fig. 11, but for the conversion of the fluence from a GRB recorded in the IBIS/ISGRI energy range 100–500 keV.

(blue) lines. They describe quite satisfactorily the drop in IBIS sensitivity to the detection of GRBs arrived at large angles to the IBIS axis. We see that it is not that large and is rather slow. Similar dependences for the SPI/ACS sensitivity to bursts have been obtained previously by Vigano and Meregetti (2009) and Pozanenko et al. (2019).

## REFERENCES

- B. P. Abbott, R. Abbott, T. D. Abbott, F. Acernese, K. Ackley, C. Adams, T. Adams, P. Addesso, et al., *Astrophys. J.* **848**, 13 (2017).
- L. Amati, *Mon. Not. Roy. Astron. Soc.* **372**, 233 (2002).
- M. V. Barkov and A. S. Pozanenko, *Mon. Not. Roy. Astron. Soc.* **417**, 2161 (2011).
- P. N. Bhat, C. A. Meegan, A. von Kienlin, W. S. Paciesas, M. S. Briggs, J. M. Burgess, E. Burns, V. Chaplin, et al., *Astrophys. J. Suppl. Ser.* **223**, 28 (2016).
- V. Bianchin, S. Mereghetti, C. Guidorzi, L. Foschini, G. Vianello, G. Malaguti, G. Di Cocco, F. Gianotti, and F. Schiavone, *Astron. Astrophys.* **536**, A46 (2011).
- R. A. Burenin, A. A. Vikhlinin, M. R. Gilfanov, O. V. Terekhov, A. Yu. Tkachenko, S. Yu. Sazonov, E. M. Churazov, R. A. Sunyaev, et al., *Astron. Astrophys.* **344**, L53 (1999).
- I. V. Chelovekov and S. A. Grebenev, *Astron. Lett.* **33**, 807 (2007).
- I. V. Chelovekov and S. A. Grebenev, *Astron. Lett.* **36**, 895 (2010).
- I. V. Chelovekov and S. A. Grebenev, *Astron. Lett.* **37**, 597 (2011).
- I. V. Chelovekov, S. A. Grebenev, and R. A. Sunyaev, *Astron. Lett.* **32**, 456 (2006).
- I. V. Chelovekov, S. A. Grebenev, and R. A. Sunyaev, in *Proc. of the 6th INTEGRAL Workshop “The Obscured Universe”* (eds. S. Grebenev, R. Sunyaev, C. Winkler), *ESA SP* **622**, 445 (2007).
- I. V. Chelovekov, S. A. Grebenev, I. A. Mereminskiy, and A. V. Prosvetov, *Astron. Lett.* **43**, 781 (2017).
- E. E. Fenimore, J. J. M. in’t Zand, J. P. Norris, J. T. Bonnell, and R. J. Nemiroff, *Astrophys. J.* **448**, L101 (1995).
- C. Fletcher, *GCN Circ.* **24185**, 1 (2019).
- S. Foley, S. McGlynn, L. Hanlon, S. McBreen, and B. McBreen, *Astron. Astrophys.* **484**, 143 (2008).
- S. Foley, S. McGlynn, L. Hanlon, S. McBreen, and B. McBreen, *Sixth Huntsville Symposium “Gamma-Ray Bursts”*, *AIP Conf. Proc.* **1133**, 362 (2009).
- D. Frederiks, D. Svinin, A. Tsvetkova, R. Aptekar, S. Golenetskii, A. Kozlova, A. Lysenko, and M. Ulanov, in *Proc. the 12th INTEGRAL conference and 1st AHEAD Gamma-ray Workshop* (Geneva, Switzerland, February 11–15, 2019, Ed. C. Ferrigno, E. Bozzo, P. von Balmoos; *astro-ph:1907.00402*) (2019).
- N. Gehrels, J. P. Norris, S. D. Barthelmy, J. Granot, Y. Kaneko, C. Kouveliotou, C. B. Markwardt, P. Meszaros, et al., *Nature* **444**, 1044 (2006).
- B. Gendre, G. Stratta, J. L. Atteia, S. Basa, M. Boër, D. M. Coward, S. Cutini, V. D’Elia, et al., *Astrophys. J.* **766**, 30 (2013).
- A. Goldstein, P. Veres, E. Burns, M. S. Briggs, R. Hamburg, D. Kocevski, C. A. Wilson-Hodge, R. D. Preece, et al., *Astrophys. J.* **848**, L14 (2017).
- D. Götz, S. Mereghetti, S. Molkov, K. Hurley, I. F. Mirabel, R. Sunyaev, G. Weidenspointner, S. Brandt, et al., *Astron. Astrophys.* **445**, 313 (2006).
- S. A. Grebenev and I. V. Chelovekov, *Astron. Lett.* **33**, 789 (2007).
- S. A. Grebenev and I. V. Chelovekov, *Astron. Lett.* **43**, 583 (2017).
- S. A. Grebenev and I. V. Chelovekov, *Astron. Lett.* **44**, 777 (2018).
- K. Hurley, *Compilation (Consolidated) Catalog of Gamma-Ray Bursts of Different Missions*, [www.ssl.berkeley.edu/ipn3/masterli.txt](http://www.ssl.berkeley.edu/ipn3/masterli.txt) (2010).
- T. M. Koshut, W. S. Paciesas, C. Kouveliotou, J. van Paradijs, G. N. Pendleton, G. J. Fishman, and C. A. Meegan, *Astrophys. J.* **463**, 570 (1996).
- C. Labanti, G. Di Cocco, G. Ferro, F. Gianotti, A. Mauri, E. Rossi, J. B. Stephen, A. Traci, and M. Trifoglio, *Astron. Astrophys.* **411**, L149 (2003).
- D. Lazzati, *Mon. Not. Roy. Astron. Soc.* **357**, 722 (2005).
- F. Lebrun, J.P. Leray, P. Lavocat, J. Crétole, M. Arqués, C. Blondel, C. Bonnin, A. Bouère, et al., *As-*

- tron. *Astrophys. J.* **411**, L141 (2003).
30. A. Martin-Carillo, V. Savchenko, C. Ferrigno, J. Rodi, A. Coleiro, and S. Mereghetti, *GCN Circ.* **24169**, 1 (2019).
  31. S. Mereghetti, D. Götz, J. Borkowski, R. Walter, and H. Pedersen, *Astron. Astrophys.* **411**, L291 (2003).
  32. I. A. Mereminskiy, S. A. Grebenev, and R. A. Sunyaev, *Astron. Lett.* **43**, 656 (2017).
  33. P. Yu. Minaev and A. S. Pozanenko, *Astron. Lett.* **43**, 1 (2017).
  34. P. Yu. Minaev, A. S. Pozanenko, and V. M. Loznikov, *Astron. Lett.* **36**, 707 (2010a).
  35. P. Yu. Minaev, A. S. Pozanenko, and V. M. Loznikov, *Astrophys. Bull.* **65**, 326 (2010b).
  36. P. Yu. Minaev, S. A. Grebenev, A. S. Pozanenko, S. V. Molkov, D. D. Frederiks, and S. V. Golenetskii, *Astron. Lett.* **38**, 613 (2012).
  37. P. Yu. Minaev, A. S. Pozanenko, S. V. Molkov, and S. A. Grebenev, *Astron. Lett.* **40**, 235 (2014).
  38. P. Minaev, A. Pozanenko, S. Grebenev, and I. Chelovekov, *GCN Circ.* **24170**, 1 (2019).
  39. A. S. Pozanenko, M. V. Barkov, P. Yu. Minaev, A. A. Volnova, E. D. Mazaeva, A. S. Moskvitin, M. A. Krugov, V. A. Samodurov, V. M. Loznikov, and M. Lyutikov, *Astrophys. J.* **852**, L30 (2018).
  40. A. S. Pozanenko, P. Yu. Minaev, S. A. Grebenev, and I. V. Chelovekov, *Astron. Lett.* **45**, 710 (2019).
  41. A. Rau, A. von Kienlin, K. Hurley, and G. G. Lichti, *Astron. Astrophys.* **438**, 1175 (2005).
  42. V. Savchenko, C. Ferrigno, E. Kuulkers, A. Bazzano, E. Bozzo, S. Brandt, J. Chenevez, T. J.-L. Courvoisier, et al., *Astrophys. J.* **848**, L15 (2017).
  43. L. Singer, *GCN Circ.* **24168**, 1 (2019).
  44. A. Tsvetkova, D. Frederiks, S. Golenetskii, A. Lysenko, P. Oleynik, V. Pal'shin, D. Svinkin, M. Ulanov, T. Cline, K. Hurley, and R. Aptekar, *Astrophys. J.* **850**, 161 (2017).
  45. P. Ubertini, F. Lebrun, G. Di Cocco, A. Bazzano, A. J. Bird, K. Broenstad, A. Goldwurm, G. La Rosa, et al., *Astron. Astrophys.* **411**, L131 (2003).
  46. G. Vianello, D. Götz, and S. Mereghetti, *Astron. Astrophys.* **495**, 1005 (2009).
  47. D. Vigano and S. Mereghetti, *POS 96*, 49 (2009) [astro-ph:0912.5329] (2009).
  48. C. Winkler, T. J.-L. Courvoisier, G. Di Cocco, N. Gehrels, A. Gimenez, S. Grebenev, W. Hermsen, J. M. Mas-Hesse, et al., *Astron. Astrophys.* **411**, L1 (2003).

*Translated by V. Astakhov*